

Structures of Apo and Product-Bound Human L-Asparaginase: Insights into the Mechanism of Autoproteolysis and Substrate Hydrolysis

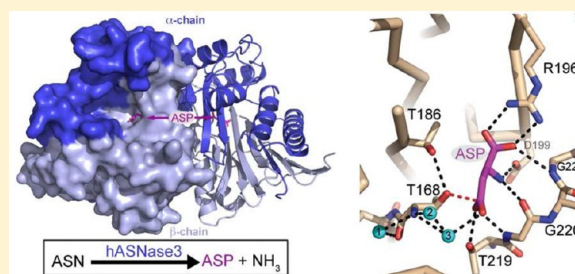
Julian Nomme,[†] Ying Su,[†] Manfred Konrad,[‡] and Arnon Lavie^{*,†}

[†]Department of Biochemistry and Molecular Genetics, University of Illinois at Chicago, Chicago, Illinois 60607, United States

[‡]Max Planck Institute for Biophysical Chemistry, Goettingen, Germany

S Supporting Information

ABSTRACT: Asparaginases catalyze the hydrolysis of the amino acid asparagine to aspartate and ammonia. Bacterial asparaginases are used in cancer chemotherapy to deplete asparagine from the blood, because several hematological malignancies depend on extracellular asparagine for growth. To avoid the immune response against the bacterial enzymes, it would be beneficial to replace them with human asparaginases. However, unlike the bacterial asparaginases, the human enzymes have a millimolar K_m value for asparagine, making them inefficient in depleting the amino acid from blood. To facilitate the development of human variants suitable for therapeutic use, we determined the structure of human L-asparaginase (hASNase3). This asparaginase is an N-terminal nucleophile (Ntn) family member that requires autocleavage between Gly167 and Thr168 to become catalytically competent. For most Ntn hydrolases, this autoproteolytic activation occurs efficiently. In contrast, hASNase3 is relatively stable in its uncleaved state, and this allowed us to observe the structure of the enzyme prior to cleavage. To determine the structure of the cleaved state, we exploited our discovery that the free amino acid glycine promotes complete cleavage of hASNase3. Both enzyme states were elucidated in the absence and presence of the product aspartate. Together, these structures provide insight into the conformational changes required for cleavage and the precise enzyme–substrate interactions. The new understanding of hASNase3 will serve to guide the design of variants that possess a decreased K_m value for asparagine, making the human enzyme a suitable replacement for the bacterial asparaginases in cancer therapy.



Asparaginases are enzymes that catalyze the hydrolysis of the free amino acid asparagine (ASN) into aspartate (ASP) and ammonia. The human genome encodes at least three enzymes that can catalyze this reaction, though the true physiological substrate of these enzymes may not be the free amino acid. One is actually called 60 kDa lysophospholipase, because of the fact that in addition to asparagine it can hydrolyze lysophospholipids.¹ This little-studied enzyme contains an N-terminal domain that is homologous to the *Escherichia coli* type I and II asparaginases, followed by several ankyrin repeats of unknown function.^{1,2} A second human enzyme that can hydrolyze ASN is aspartylglucosaminidase (hAGA). The main function of this lysosomal enzyme is to remove carbohydrate groups linked to asparagine, as a final step in the degradation of cell surface glycoproteins. Defects in hAGA are the cause of aspartylglucosaminuria (AGU), which is an inborn lysosomal storage disease.³ The third enzyme with asparaginase activity, and the focus of this report, is indeed called L-asparaginase (also known as hASRGL1/ALP⁴/CRASH⁵), despite the fact that it can also hydrolyze isoaspartyl peptide linkages,⁶ which are a common source of protein damage.⁷ This enzyme is homologous to the *E. coli* type III asparaginase, and therefore, we refer to it as human asparaginase 3 (hASNase3).

Type III asparaginases belong to the N-terminal nucleophile (Ntn) family of hydrolases.⁸ Interestingly, the aspartylglucosaminidase hAGA also belongs to this family. Ntn enzymes are produced as a single polypeptide that must undergo intramolecular cleavage to attain catalytic activity. The cleavage reaction is an autocatalytic process, in which the side chain of a threonine, serine, or cysteine (depending on the specific Ntn enzyme⁹) residue attacks the carbonyl group of the preceding amino acid to form a covalent intermediate. The intermediate subsequently undergoes hydrolysis to yield the peptide-cleaved enzyme. This type of activation by autoproteolysis is different from that which occurs in proenzymes such as trypsin. In proenzymes, peptide bond cleavage typically functions to displace a short N-terminal inhibitory segment. In contrast, in Ntn enzymes, cleavage occurs around midway of the peptide sequence, and the resulting two chains, termed α - and β -chains, remain intact to form a single functional unit. The purpose of the cleavage reaction is to release the amino group of the Thr, Ser, or Cys residue from being involved in peptide bond

Received: June 28, 2012

Revised: August 2, 2012

Published: August 3, 2012

formation to being N-terminally exposed in the β -chain, which can then attack its substrate. Thus, the Thr, Ser, or Cys residue plays dual roles, first in initiating the maturation reaction of the enzyme into its active state and then in catalyzing hydrolysis of free asparagine or asparagine derivatives.

Human hASNase3 differs from most studied Ntn enzymes by undergoing a very slow self-cleavage reaction. For example, whereas the *E. coli* type III asparaginase is purified as the fully cleaved form,¹⁰ sodium dodecyl sulfate–polyacrylamide gel electrophoresis of purified recombinant hASNase3 expressed in *E. coli* shows a predominate single band corresponding in size to the uncleaved enzyme, with only weak bands for the lower-molecular weight α - and β -chains of the cleaved state. Incubation of hASNase3 in a buffer containing NaCl and Tris-HCl (pH 7.5) increases the proportion of the cleaved state at a very slow rate, as observed by us (manuscript submitted) and others.⁶ The uncleaved enzyme crystallizes under several salt-containing conditions, such as malonate, citrate, and ammonium sulfate. Diffraction data collected from these crystals show that the extent of protein cleavage (i.e., the peptide bond break between Gly167 and Thr168) is dependent on the age of the crystals, with fresh crystals being uncleaved and older crystals (>90 days) being predominantly cleaved. In our earlier work, we made the unexpected discovery that the amino acid glycine very selectively accelerates the cleavage reaction (manuscript submitted).

In addition to hydrolyzing ASN and diverse ASN-linked substrates, asparaginases play a prominent role in cancer chemotherapy.¹¹ Bacterial asparaginases, specifically the *E. coli* type II enzyme (trade name Elspar), its conjugate with polyethylene glycol (PEG), Oncospar, and that from *Erwinia chrysanthemi* (Erwinase), are key agents in inducing remission of acute lymphoblastic leukemia and lymphoblastic lymphoma. Note that these clinically used asparaginases are not Ntn enzymes and have a structure completely different from that of hASNase3;¹² for a discussion of different types of asparaginases, see the recent review by Michalska et al.¹³ The clinical success of asparaginase therapy is attributed to the rapid and complete depletion of the amino acid ASN in plasma.¹⁴ Serum contains a steady-state level of $\sim 50 \mu\text{M}$ ASN.¹⁵ Although ASN is not an essential amino acid, several tissues (thymus, T-cells, etc.) depend on extracellular sources of ASN for their metabolic needs. ASN is a crucial amino acid for protein, DNA, and RNA synthesis,¹⁶ and its requirement is cell cycle-specific for the G1 phase of cell division.¹⁷ While a de novo pathway for ASN synthesis exists (via ASN synthetase), many cancer cells such as leukemic cells are dependent on the availability of extracellular ASN. Hence, ASN depletion achieved upon administration of the bacterial asparaginases interferes with the metabolic status of the cancer cell and ultimately results in apoptosis.¹⁸

However, clinical use of these drugs is complicated by an immune response against the bacterial enzymes. Use of the Oncospar version attempts to limit this immunogenicity, based on the observation that foreign proteins covalently linked to PEG may mask immunogenic epitopes. However, eventually enzyme-specific or even PEG-specific antibodies are elicited,¹⁹ which cause a variety of adverse effects, including hypersensitivity and anaphylactic shock. Moreover, these bacterial asparaginase-specific antibodies inactivate the enzyme and promote its clearance, negating its therapeutic potential. To eliminate the immunogenicity of the enzymes, we propose use of human asparaginases in lieu of bacterial enzymes. However, intrinsically none of the three human asparaginases has the

required kinetic property (low micromolar K_m) adequate for replacing bacterial asparaginases. Hence, we commenced the study of hASNase3 with the ultimate goal of engineering a low- K_m ASN variant suitable for use in humans. As a first step toward this goal, we determined the crystal structures of hASNase3 in various states. Here we present the uncleaved and cleaved enzyme states, either without substrate or in complex with the product L-aspartate. Together, these structures reveal details of the substrate–enzyme interactions, inform us about the specific roles of active site residues, and provide insight into the mechanism of autocleavage and ASN hydrolysis.

MATERIALS AND METHODS

Cloning of Human hASNase3. The open reading frame (ORF) of hASNase3 (UniProt entry Q7L266, also called human asparaginase-like protein 1, hASRGL1, ALP, or CRASH), consisting of 927 bp, was amplified via polymerase chain reaction (PCR) using as a template cDNA from a human skin and meninges cDNA library (Source Bioscience). NdeI and BamHI sites were incorporated into the oligonucleotides targeting the 5' and 3' ORF ends, respectively. The PCR product was gel-purified, digested with NdeI and BamHI-HF (New England Biolabs), and ultimately ligated overnight at 16 °C into the pET14b-SUMO vector using T4 DNA ligase. The ligation mixture was used to transform DH5 α *E. coli* cells. Positive clones were determined following restriction digestion with NdeI and BamHI-HF, and finally, the gene insert was sequenced. The final construct includes an N-terminal six-histidine tag, followed by SUMO (small ubiquitin modifier; yeast protein Smt3p of 101 residues) tag, which has been proven to improve heterologous protein solubility and stability. For bacterial expression, the *E. coli* BL21(DE3) C41 strain was transformed with the hASNase3 plasmid.

Expression and Purification of hASNase3. Two liters of 2YT medium was inoculated with a starter culture of *E. coli* BL21(DE3) C41 carrying the hASNase3 plasmid. When the cultures reached an optical density at 600 nm in the range of 0.6–0.8, the temperature was reduced from 37 to 18 °C, 0.5 mM IPTG was added to induce expression, and cells were left to grow overnight. Cells were spun down and then lysed by sonication [lysis buffer (50 mM Tris-HCl (pH 7.5), 500 mM NaCl, 10% glycerol, 1% Triton 100, and 1 mM PMSF)], and the lysate was cleared by ultracentrifugation (1 h at 33K rpm). The supernatant was loaded onto a 5 mL His-Trap HP Ni Sepharose column (GE Healthcare), washed with 150 mL of a buffer containing 25 mM Tris-HCl (pH 7.5), 500 mM NaCl, and 10 mM imidazole. Further washing was done with a similar buffer that contains 25 mM imidazole. Elution of the protein was accomplished with a buffer containing 250 mM imidazole, with a yield of 290 mg of total protein (Bradford assay). At this stage, SUMO protease was added (1:200 weight ratio) to cleave the His-SUMO tag from hASNase3 and the protein left to dialyze overnight to remove the imidazole. The cleaved protein was put back onto the His-Trap column, with hASNase3 coming out in the flow through. After protein had been concentrated to a volume of 5 mL (22 mg/mL), the sample was injected onto a S-200 gel filtration column (GE Healthcare) pre-equilibrated with 25 mM Tris-HCl (pH 7.5), 200 mM NaCl, and 2 mM DTT. The protein eluted as two peaks: a minor peak that would correspond to the dimer and a major peak that would correspond to the monomer. The monomer peak was pooled, concentrated to 38 mg/mL, aliquoted, and stored at -80°C .

Table 1. Data Collection and Refinement Statistics

	sulfate complex	malonate complex	partially cleaved ASP complex	fully cleaved ASP complex
PDB entry	4GDU	4GDT	4GDV	4GDW
		Data Collection ^a		
X-ray source and detector	R-Axis IV++	R-Axis IV++	R-Axis IV++	R-Axis IV++
wavelength (Å)	1.5418	1.5418	1.5418	1.5418
temperature (K)	93	93	93	93
resolution (Å)	2.13 (2.13–2.25)	1.85 (1.85–1.96)	1.75 (1.75–1.80)	1.84 (1.84–1.96)
no. of reflections				
observed	91279	217177	339360	143931
unique	26285	48285	59545	50184
completeness (%)	79.4 (53.5)	94.7 (69.5)	99.2 (96.1)	97.4 (88.4)
R _{sym} (%)	6.7 (32.5)	4.7 (24.9)	6.1 (31.4)	3.9 (42.1)
average I/σ(I)	12.81 (2.89)	18.44 (2.58)	17.35 (2.02)	16.94 (2.10)
space group	P6 ₅	P6 ₅	P6 ₅	P6 ₅
unit cell (Å)				
a = b	59.22	59.46	59.50	59.67
c	298.48	298.90	299.50	298.72
		Refinement		
refinement program	Refmac5	Refmac5	Refmac5	Refmac5
twinning fraction	0.531	0.506	0.503	0.501
R _{cryst} (%)	16.9	16.2	16.1	17.1
R _{free} (%)	22.3	20.5	19.1	21.6
resolution range (Å)	51.3–2.13	51.5–1.85	51.5–1.75	51.7–1.84
no. of protein molecules per asymmetric unit	2	2	2	2
no. of atoms				
protein (protA, protB)	2132, 2149	2186, 2172	2196, 2165	2165, 2165
malonate/SO ₄ ²⁻	–/13	7/–	–/–	–/–
aspartate	–	–	2 × 9	2 × 9
water molecules	212	251	263	259
Na ⁺	2 × 1	2 × 1	2 × 1	2 × 1
I ⁻	4	–	–	–
rmsd from ideal				
bond lengths (Å)	0.010	0.011	0.010	0.009
bond angles (deg)	1.30	1.28	1.27	1.22
average B factor (Å ²)				
protein (protA, protB)	27.3, 27.2	22.9, 23.4	12.6, 12.9	25.4, 25.5
malonate/SO ₄ ²⁻	–/30.1	23.4/–	–/–	–/–
aspartate	–	–	20.5, 22.1	19.7, 26.5
water molecules	25.0	24.4	17.5	28.1
Na ⁺	30.2, 24.6	25.3, 27.5	8.4, 13.2	21.2, 47.5
I ⁻	51.6	–	–	–
Ramachandran plot (%)				
most favored regions	88.8	89.5	90.8	89.9
additionally allowed regions	10.3	9.9	8.6	9.7
generously allowed regions	0.2	0.2	0.4	0.0
disallowed regions	0.6	0.4	0.4	0.4

^aData for the last shell in parentheses.

Crystallization of hASNase3. Purified hASNase3 was subject to crystallization condition screening, and crystals of hASNase3 (without added amino acid) were obtained under several conditions with salts as precipitants (e.g., citrate, malonate, and ammonium sulfate). Optimization of JCSG +Suite (Qiagen) condition 69 [2.4 M sodium malonate (pH 7)] to 2.2 M malonate resulted in large crystals that diffracted beyond 1.6 Å. For setups, 1 μL of hASNase3 at 38 mg/mL [in 25 mM Tris (pH 7.5), 200 mM NaCl, and 2 mM DTT] was mixed with 1 μL of the reservoir on a glass coverslip and left to undergo vapor diffusion using the hanging drop method at 20 °C. Crystals appeared after ~5 days. We also obtained crystals in JCSG+Suite condition 23 (1.6 M sodium citrate) and

ammonium sulfate Suite (Qiagen) condition 9 (0.2 M ammonium iodide and 2.2 M ammonium sulfate).

Crystals used in this study were grown under the malonate condition, except for one substrate-free structure obtained from crystals grown in ammonium sulfate. Electron densities resulting from crystals grown under these three different conditions revealed precipitant molecules occupying the substrate binding site (see below). To solve this precipitant-competition problem for the purpose of obtaining the structure of hASNase3 in complex with L-aspartate (ASP), crystals grown in malonate were transferred to a 2 M aspartate (pH 7.5), 20% glycerol solution for 5 min. To obtain the fully cleaved structure in complex with ASP, we first transferred crystals to a 2 M

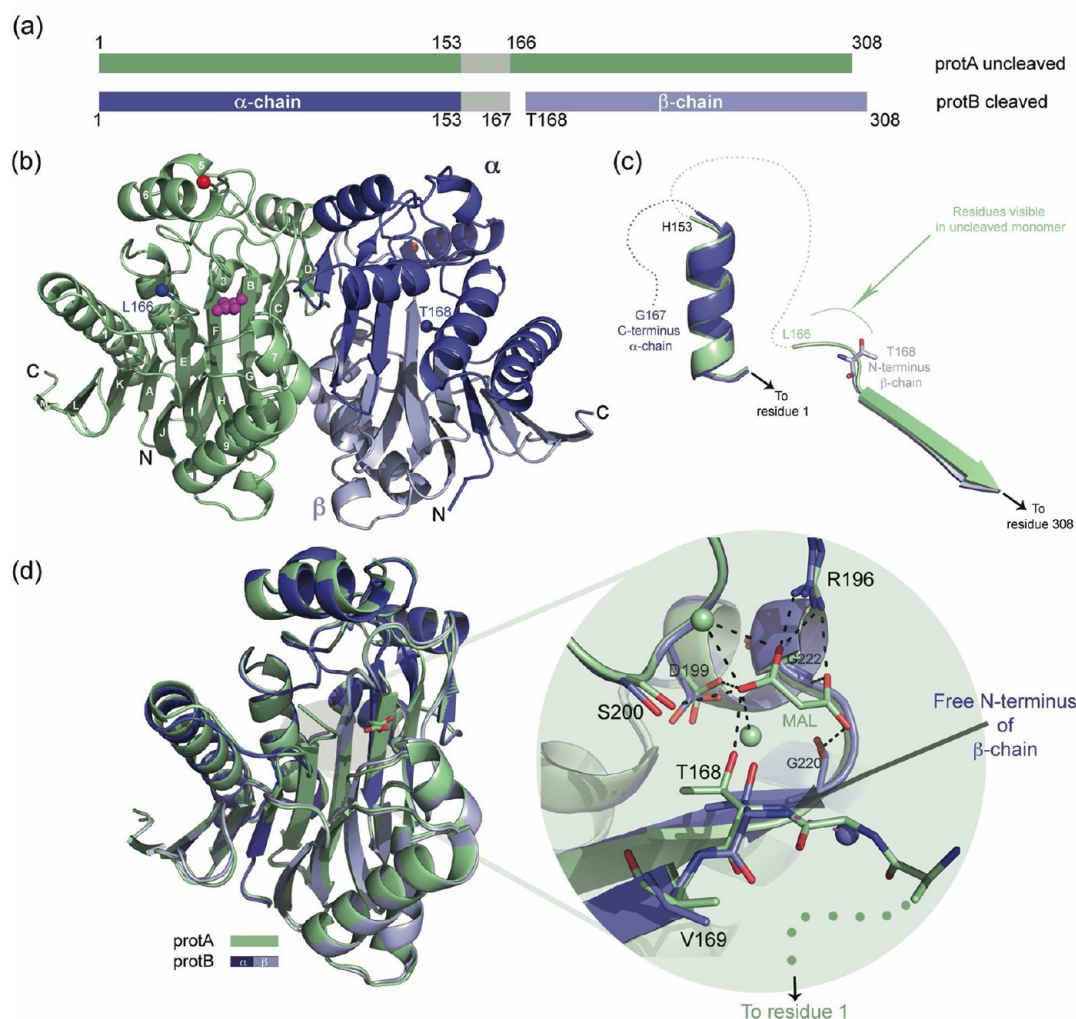


Figure 1. Cleaved vs uncleaved structures of substrate-free hASNase3. (a) Schematic representation of hASNase3 as observed in the dimeric asymmetric unit of the malonate complex. The entire uncleaved protomer (protA) is colored green, except for regions lacking interpretable electron density, which are colored gray. The cleaved protomer (protB) is colored dark and light blue, representing the α - and β -chains, respectively. (b) Ribbon diagram of the hASNase3 dimer, colored as in panel a, with the secondary structure elements annotated. The protA active site-bound malonate is colored magenta. Red and blue spheres represent the terminal amino acids visible in the flexible H153–T168 loop. (c) Overlay of the uncleaved (protA) and cleaved (protB) protomers, focused on the structural elements spanning the cleavage site. See the text for details. (d) An overlay as in panel c, depicting the entire molecule, demonstrates that the uncleaved and cleaved conformations are essentially identical. The right panel is a close-up of the cleavage site. The bound malonate (MAL) is shown as sticks, and black dashed lines represent interactions with the enzyme and solvent (green spheres). Upon cleavage, the space previously occupied by G167 is taken by a water molecule (blue sphere).

glycine solution (pH 7.5) for 1 min and then to the 2 M ASP (pH 7.5), 20% glycerol solution for 5 min.

Data Collection and Structure Solution of hASNase3.

Diffraction data were collected using the in-house X-ray source (Rigaku RU-200 rotating anode) with a R-Axis IV++ image plate detector. Data were processed using XDS.²⁰ The structure was determined by molecular replacement (Molrep²¹ CCP4) using the bacterial asparaginase EcAIII as a starting model [Protein Data Bank (PDB) entry 2ZAK] and refined with Refmac5.²² Structure figures were made with PyMol. All crystals were perfectly twinned, with the true space group being $P6_3$ (apparent space group, $P6_322$), and contained two copies of hASNase3 in the asymmetric unit. Data collected on freshly grown crystals showed the uncleaved state of the enzyme, whereas data for older crystals showed the cleaved state. Under all the crystallization conditions mentioned above, the salt used as a precipitant was observed at the enzyme active site. Attempts to soak in the product ASP, even at a concentration

of 100 mM, failed to result in density for this amino acid. We interpret this as being due to competition by the precipitant salt. Hence, to obtain the ASP complex, we transferred crystals into a high-concentration ASP solution that acted to stabilize the crystals and to provide the source of the amino acid binding at the active site.

RESULTS AND DISCUSSION

Cleaved versus Uncleaved States of hASNase3. We determined two amino acid-free hASNase3 structures, one from crystals grown with ammonium sulfate as the precipitant (at 2.13 Å resolution) and another from crystals grown in malonate (1.85 Å). Data collection and refinement statistics are listed in Table 1. Regardless of the precipitant used, the crystals adopted the same space group and unit cell dimensions, contained two molecules in the asymmetric unit, and were invariably twinned. Additionally, in every case we observed a precipitant molecule bound at the active site (see below). This is not surprising

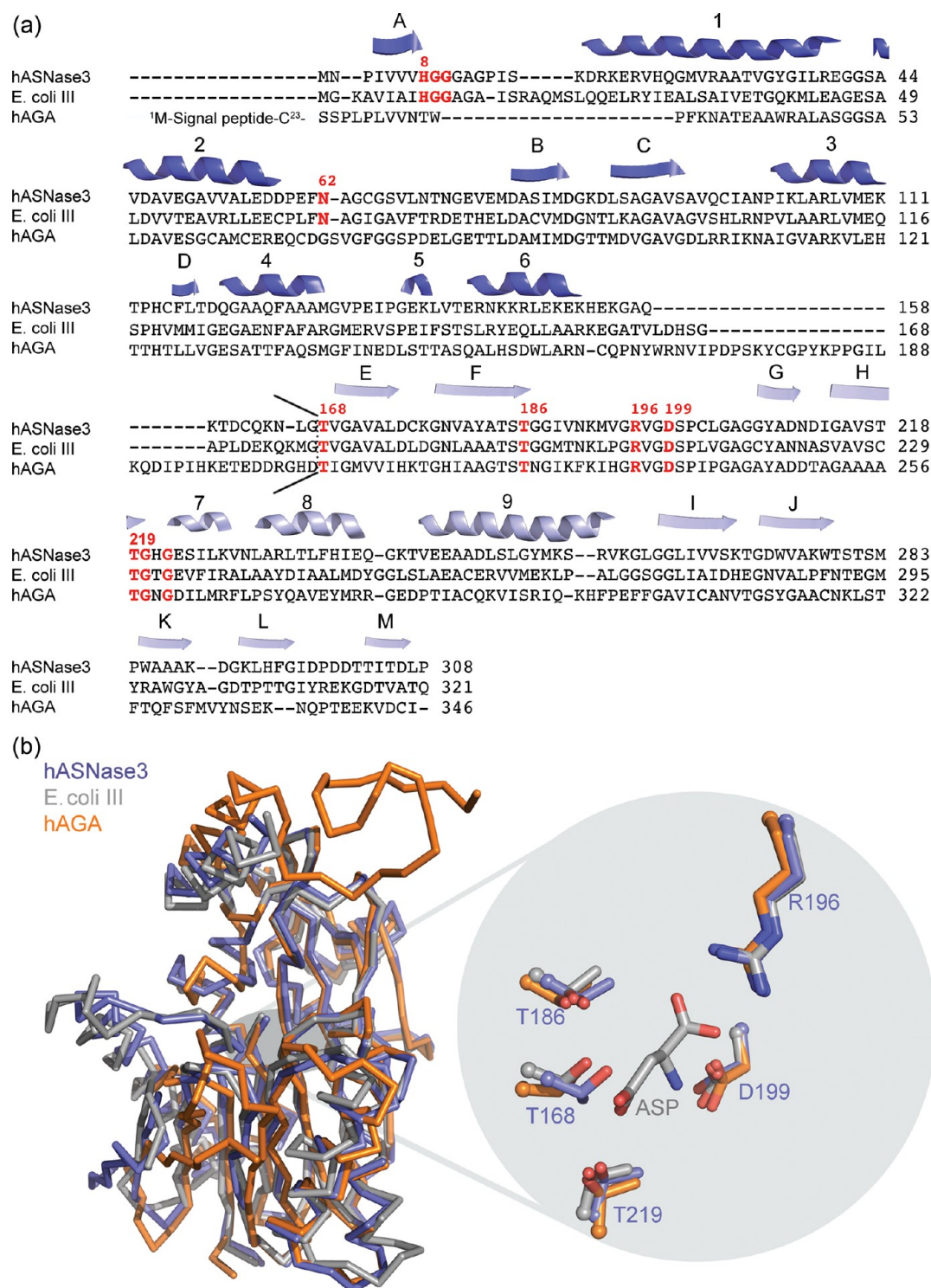


Figure 2. Sequence and structure alignment of hASNase3, *E. coli* type III, and hAGA. (a) Sequences of hASNase3 (ASGL1_HUMAN), *E. coli* type III (IAAA_ECOLI), and hAGA (ASPG_HUMAN) aligned using Clustal W. The first 23 amino acids corresponding to the hAGA signal peptide are not shown. hASNase3 secondary structure elements are presented and annotated (α - and β -chains in dark and light blue, respectively). Conserved active site residues are colored red. The cleavage site for these Ntn enzymes is marked by a black line. (b) Overlay of hASNase3, *E. coli* type III (PDB entry 2ZAL) and hAGA (PDB entry 1APZ), colored blue, gray, and orange, respectively. The right panel is a close-up of the highly conserved active site threonines and aspartic acid/arginine residues (hASNase3 numbering). Depicted ASP molecule (gray sticks), as seen in the *E. coli* type III structure.

because of the similar structural properties of the precipitants and the substrate ASN.

Human ASNase3 is a homodimer, and its structure obtained from crystals grown in ammonium sulfate revealed the

uncleaved state of the enzyme in both protomers. We could model several sulfate molecules, with one sulfate at the active site (hence the designation sulfate complex). Likewise, the structure from the malonate condition contained the

predominantly uncleaved state in protomer A (protA; modeled as 75% uncleaved and 25% cleaved). In contrast, protomer B (protB) of the malonate-grown crystal was observed to be 100% cleaved. We could model a malonate molecule bound at the active site of protA (hence the designation malonate complex) but not in protB. Apart from localized structural differences due to cleavage of protB, these substrate-free structures from the different precipitants are basically identical (rmsd of 0.27 Å over 529 C α atoms). A comparison of all uncleaved protomers discussed here is presented in Figure S1 of the Supporting Information. On the basis of the fact that the amino acid-free structure of the malonate complex was of higher resolution, and because it allows us to compare the uncleaved versus cleaved state from the same crystal (Figure 1a), our analysis of the amino acid-free structure is focused on this data set.

The amino acid-free hASNase3 structure is presented as a ribbon diagram of the dimeric asymmetric unit (Figure 1b). However, it is unclear if this dimer (interface area of ~ 1800 Å²; PISA server²³) is indeed the physiological oligomeric state for hASNase3 because the gel filtration elution profile shows a major peak corresponding to the monomer, and only a minor peak corresponding to the dimer. This is similar to the observation made with the homologous glycosylasparaginase from *Flavobacterium meningosepticum*, where only a monomer was observed using gel filtration.²⁴ On the other hand, all known structures of Ntn enzymes, including the latter one, reveal a similar dimeric arrangement, suggesting that the dimer is physiologically relevant. Because active site residues originate from a single protomer and kinetic studies have not revealed cooperativity, dimer formation may serve only a stabilizing role.

The uncleaved protA of hASNase3 (green in Figure 1) has a malonate molecule (magenta in Figure 1b) at the active site, whereas the active site of the uncleaved protB (dark and light blue, representing the α - and β -chains, respectively) is occupied by solvent molecules. The reason for this difference is not clear and does not seem to be a result of the cleavage status. The determination of cleaved versus uncleaved enzyme state was made on the basis of two criteria. The first is the presence or absence of electron density extending in the N-terminal direction from Thr168. In this amino acid-free structure, for protA we could model the preceding Gly167 and the main chain atoms of Leu166 (at 75% occupancy), but not beyond (Figure 1c and Figure 1d, close-up). In contrast, for protB the electron density did not extend beyond Thr168, and hence it was designated as cleaved. The second criterion was the ability of the conformation of Gly9, which we observe for the first time for Ntn enzymes, to flip depending on the cleavage state of the enzyme (Figure S2 of the Supporting Information). Interestingly, a glycine at this position is common for Ntn enzymes (Figure S3 of the Supporting Information), suggesting that this glycine-enabled peptide flip is important for stabilizing the cleaved state. We discuss the possible function of this region in the section detailing the cleavage mechanism.

Despite the fact that protA was uncleaved, residues spanning His153 and Leu166 lacked clear electron density (Figure 1c). This observation is consistent with that made with other Ntn enzymes^{25,26} that even in the uncleaved state (in those cases, requiring mutants devoid of cleavage ability) several residues at the tip of the α -chain cannot be modeled, suggesting that this region is intrinsically disordered. In the cleaved protB, we also could trace the α -chain only as far as His153, demonstrating that after cleavage, the most C-terminal residues of the α -chain

(residues 154–167) do not adopt a defined conformation. Whereas the two protomers differ in their cleavage state and in the presence of the precipitant molecule bound at the active site, their overall structure is nearly identical, with an rmsd of 0.31 Å over 267 atoms (Figure 1d). Hence, cleavage does not induce a significant conformational change, with the most pronounced differences between the cleaved and uncleaved enzyme being the positioning of Thr168 (Figure 1d, close-up), which differs by 0.6 Å (C α atom), and the aforementioned conformation of Gly9. In the cleaved state, a water molecule occupies the position previously taken by Gly167. Of course, the most significant aspect of the cleavage is the liberation of the amino group of Thr168, which then becomes the N-terminal residue of the β -chain and can now participate in the catalysis of ASN hydrolysis. To the best of our knowledge, this is the first structure of an uncleaved Ntn enzyme obtained without resorting to mutations that abolish or slow self-cleavage, an accomplishment made possible by the intrinsically slow cleavage rate of hASNase3.

Comparison to *E. coli* Type III Asparaginase and hAGA. Both human ASNase3 and AGA are homologues of the *E. coli* type III asparaginase (Figure 2a and Figure S3 of the Supporting Information). In terms of overall structure, hASNase3 is highly similar to the *E. coli* type III asparaginase²⁵ [rmsd of 0.52 Å over 228 atoms (Figure S4a of the Supporting Information)] yet has significant structural differences with its human homologue AGA²⁷ [rmsd of 1.0 Å over 175 atoms (Figure S4b of the Supporting Information)], as clearly seen in the overlay of the three enzymes (Figure 2b). This mirrors the greater degree of sequence homology between hASNase3 and the *E. coli* enzyme (37.5% identical, 64.5% similar, over a 301-residue overlap) compared to that between hASNase3 and hAGA (29.2% identical, 60.6% similar, over a 277-residue overlap).

The hallmark of these three asparaginases is the presence of three threonine residues at the active site; on the basis of hASNase3 numbering, these are Thr168, Thr186, and Thr219 (Figure 2a). Also conserved are Arg196 and Asp199 that bind the substrate (see below). Not surprisingly because of high degree of structural and sequence homology between hASNase3 and *E. coli* type III asparaginase, these residues occupy identical relative positions in the active site (Figure 2b, close-up). More remarkable is that these residues also line up exceptionally well with those from the less similar hAGA, demonstrating conserved active site architecture.

Cleaved and Uncleaved ASP Complex Structures. For insight into how hASNase3 binds its substrate, we sought to determine the structure of the enzyme with the product ASP. Hence, preformed crystals were transferred to a solution containing the crystallization mix and the amino acid (up to 100 mM). However, diffraction data collected on such crystals failed to show electron density for the ASP, instead showing density consistent with the precipitant used in the crystallization. We attribute this to the fact that the precipitant (e.g., malonate, citrate, or ammonium sulfate at >1.5 M) also binds to the active site and thus outcompetes the soaked-in ASP. To overcome this problem, we transferred preformed crystals into a 2 M ASP solution (pH 7.5), with the rationale that such a high amino acid concentration would substitute the precipitant salt in stabilizing the crystal and at the same time provide the ASP that binds at the active site. Indeed, a data set collected on a crystal soaked into ASP [1.75 Å resolution (Table 1)] did

show a clear electron density for the amino acid, which was present in both protomers.

Recapitulating the observation made with the malonate complex structure, in this ASP complex we observed that protA was only partially cleaved (modeled as 50% uncleaved and 50% cleaved) and protB was fully cleaved, and that the cleaved and partially cleaved protomers have a nearly identical structure (rmsd of 0.34 Å for 288 atoms) with differences limited to the cleavage site (Figure 3a). This structure, designated as the

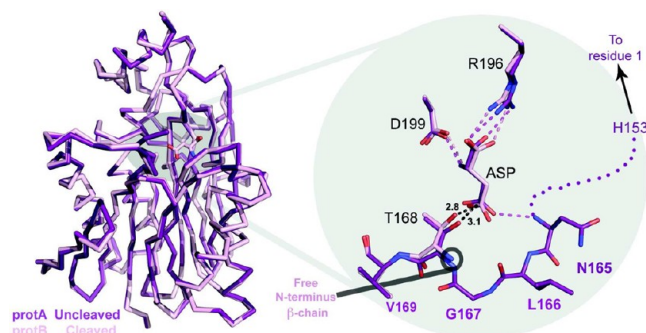


Figure 3. Comparison of the ASP-bound enzyme conformation in the cleaved and uncleaved states. α trace representation of superimposed hASNase3 protA (uncleaved, magenta) and protB (cleaved, pink) as observed in the partially cleaved ASP complex structure. Aspartate (ASP) is represented as sticks. The right panel highlights the active site residues binding the ASP (colored dashed lines). Uncleaved protA residues surrounding T168 are shown, with the dotted line representing residues lacking interpretable electron density. Cleaved protB residues T168 and V169 are also shown. Note the small change in the position of T168 upon cleavage.

partially cleaved ASP complex, demonstrates that the product ASP, and by analogy the substrate ASN, can bind to the enzyme irrespective of its cleavage status. For the partially cleaved protA, we could model three residues that precede Thr168, but the residues linking His153 and Asn165 had no interpretable electron density (Figure 3a, close-up). In the cleaved protomer (protB), we could not build a model beyond His153 of the α -chain. This shows that the presence of product (and presumably of substrate as well) does not induce order to the C-terminal residues of the α -chain (residues 154–167), in either the uncleaved or the cleaved state.

This crystal structure allows a direct comparison of ASP binding to the uncleaved and cleaved states of hASNase3 (Figure 3, close-up) for understanding the essentiality of cleavage for asparaginase activity. The hydrolysis of ASN is thought to commence with the attack of the Thr168 hydroxyl group on the amino acid's side chain carbonyl group. Figure 4 presents a schematic of the hASNase3 asparaginase reaction mechanism, adapted from that previously suggested for hAGA.²⁸ The amino group of Thr168 (free in the cleaved state) acts to activate its hydroxyl group to attack the ASN side chain (panel I), with the negatively charged tetrahedral intermediate being stabilized by the oxyanion hole composed of Thr219 and Gly220 (panel II). Breakdown of the intermediate releases ammonia (panel III) with the amino acid remaining covalently bound to Thr168. The water molecule observed sandwiched between the amino group of Thr168 and the side chain amino group of ASN could act as a proton donor to the leaving NH_2 group. Hydrolysis (panel IV) would likely build a very similar tetrahedral intermediate (panel V) to yield the free enzyme and the product ASP (panel VI). In our structures, in both the uncleaved and cleaved states, the

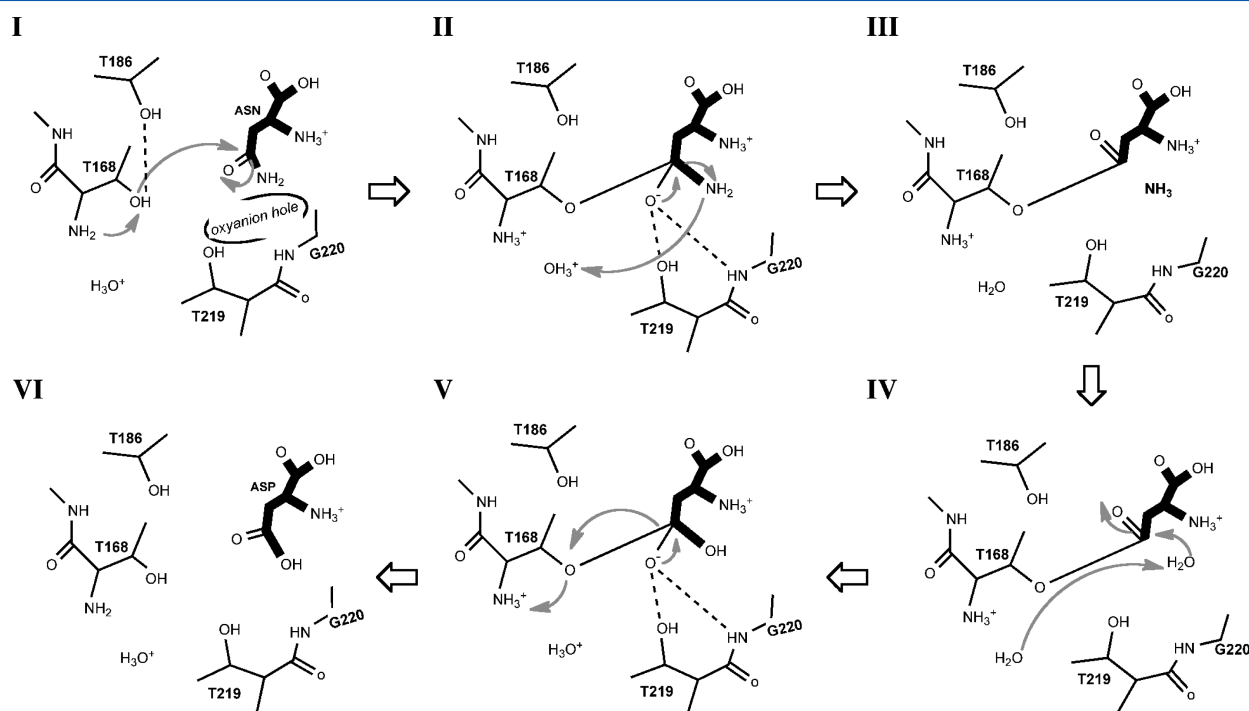


Figure 4. hASNase3 reaction mechanism. In the enzyme's cleaved state, the amino group of Thr168 acts to activate its side chain for attack on the ASN side chain (I). The ensuing negative charge of the tetrahedral intermediate is stabilized by the oxyanion hole composed of Thr219 and Gly220 (II). The water molecule flanking the Thr168 amino group and the ASN side chain could act as a proton donor for the leaving group. After release of ammonia (III), a water molecule hydrolyzes the covalent intermediate (IV) via a similar tetrahedral state (V) to yield the product ASP and the free enzyme. Reaction mechanism adapted from Tikkanen et al.²⁸ Experimentally derived distances between ASP and the enzyme are shown in Figure 5b.

Thr168 hydroxyl group is within 2.8–3.1 Å of the ASP side chain carbonyl group. Hence, improper substrate positioning can be ruled out as the reason for the lack of asparaginase activity of the uncleaved enzyme and supports the catalytic role of the Thr168 amino group as detailed in the reaction schematic.

Product Binding to Fully Cleaved hASNase3. To determine the structure of fully cleaved hASNase3 in complex with ASP, we took advantage of our discovery that the amino acid glycine promotes the cleavage reaction (manuscript submitted). Hence, a preformed crystal was first transferred into a 2 M glycine solution (pH 7.5) and incubated for ~4 min to promote cleavage. Subsequently, the crystal was transferred to a 2 M ASP solution (pH 7.5) and, after a short soak, frozen in liquid nitrogen. Indeed, diffraction data (1.84 Å, Table 1) from this crystal revealed full cleavage of both protomers and the presence of an ASP molecule (Figure 5a) in each active site of the dimeric enzyme (hence, the designation fully cleaved ASP complex). The amino acid is bound at the active site through several polar interactions (Figure 5b,c). (i) The α -carboxylic moiety forms a bidentate salt bridge with the side chain of Arg196, as well as interacting with the main chain NH group of Gly222. (ii) The amino moiety of ASP is stabilized by the side chain of Asp199 and by the carbonyl of Gly220. (iii) The carboxylic side chain of ASP is at interacting distance to the side chain of Thr219 and the NH group of Gly220. Because both of these moieties can function as hydrogen bond donors, they would interact with the oxygen atom of ASN's side chain, not its amino group. This would orient the side chain such that the leaving group of the reaction, the amino group, is not encumbered by interactions with the enzyme. (iv) Most notable in terms of the reaction mechanism, the ASP carboxylic side chain is 2.2 Å from the hydroxyl of Thr168. In fact, this hydroxyl group is only 2.6 Å from the ASP carboxylate carbon atom (red dashed line in Figure 5c). The asparaginase reaction is dependent on the free amino group of Thr168, which is thought to be required, directly or via a water molecule,²⁹ to activate the Thr168 hydroxyl group (see the proposed mechanism in Figure 4).²⁸ Of the water molecules observed closest to the Thr168 amino group (numbered 1–3 in Figure 5c), none acts to bridge the amino group or the Thr168 hydroxyl group. Further inspection of this region reveals that nearby water molecules are stabilized by the side chain of Asn62, which is in turn positioned by interactions with Gly187 and Gly188 (Figure 5d). Hence, in the case of hASNase3, it seems that the amino group of Thr168 directly activates its hydroxyl group (distance of 2.9 Å) and that nearby water molecules, held in position by Asn62, can help to shuttle the proton.

Asn62 is a part of the sodium-binding loop (residues 55–65), a feature observed previously for this asparaginase family,³⁰ that would anchor its main chain position. Inspection of Ntn-type enzyme sequences shows that Asn62 and the tandem glycine residues following Thr186 (Gly187 and Gly188) are highly conserved (Figure S3 of the Supporting Information). This supports the model in which these conserved residues act to position water molecules near the amino group of Thr168, whose function is to stabilize the protonated amine group once it has abstracted the proton from the Thr168 hydroxyl group (Figure 4, panels I and II). Interestingly, the homologous asparagine residue in the *E. coli* Type III asparaginase (Asn67) has been implicated in the cleavage reaction,³¹ suggesting a dual cleavage and asparaginase role for this side chain.

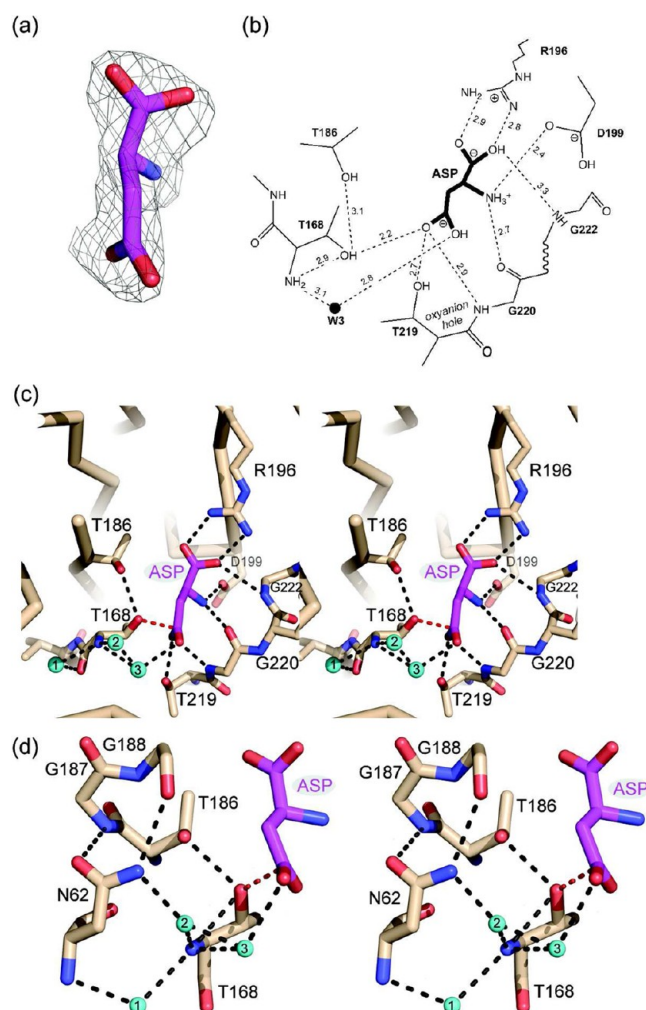


Figure 5. Fully cleaved hASNase3 structure in complex with ASP. (a) ASP $2F_o - F_c$ omit map. ASP conformation is defined in unbiased electron density that was calculated before the ligand was built in (contour level of 1σ). (b) Schematic representation of ASP bound at the hASNase3 active site. Numbers represent distances in angstroms. W3 is one of three water molecules in the vicinity of the Thr168 amino group. (c) Stereoview of the hASNase3 active site from the fully cleaved ASP complex structure (tan). Black dashed lines indicate interaction with ASP (magenta) and solvent molecules (labeled 1–3). The red dashed line shows the distance between the Thr168 hydroxyl group and the ASP β -carboxylate carbon atom (2.6 Å). (d) Stereoview of the region around N62 and T168, with interactions denoted by dashed lines. The N62 side chain, positioned by interactions with conserved G187 and G188, acts to stabilize water molecules (labeled 1–3) in the vicinity of the Thr168 amino group.

Implication for the Autocleavage Mechanism. In the three crystal structures of hASNase3 analyzed here (for the sake of simplicity, we omit the sulfate complex), we observe a total of two protomers in the uncleaved state (protAs of the malonate and partially cleaved ASP complex) and four protomers in the cleaved state (protBs of the above, plus both protomers of the fully cleaved ASP complex). What can these structures tell us about the autocleavage mechanism? Just as the side chain of the N-terminal threonine of the β -chain is required for ASN hydrolysis, this side chain is also required to initiate the cleavage process. It does this by attacking the carbonyl group of the preceding amino acid, Gly167 in the case of hASNase3. However, in our uncleaved structures, the

distance between the Thr168 hydroxyl group and the carbonyl carbon atom of Gly167 is too large (4.0 Å) in the case of the uncleaved ASP complex protomer (Figure 6a). This suggests

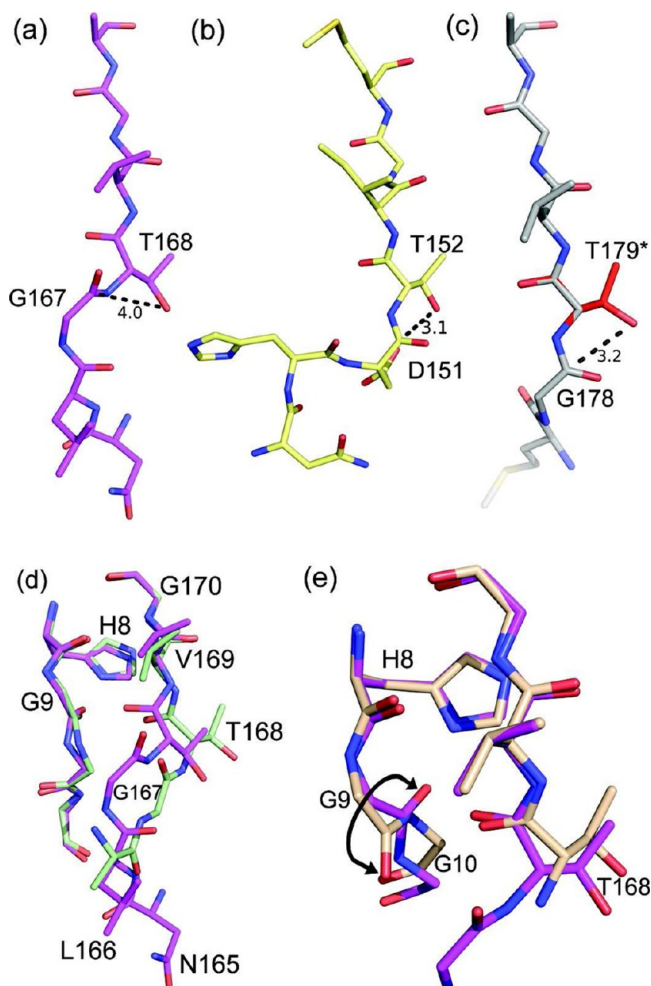


Figure 6. hASNase3 cleavage requires flexibility at the cleavage site. Structural comparison of three mechanistically related asparaginases in their precleaved state. (a) hASNase3 (partially cleaved ASP complex; uncleaved protA) cleavage site. The distance from the Gly167 carbonyl carbon atom to the Thr168 hydroxyl group is 4.0 Å. (b) *F. meningosepticum* glycosylasparaginase (PDB entry 9GAF) cleavage site. The distance from the Asp151 carbonyl carbon atom to the Thr152 hydroxyl group is 3.1 Å. (c) *E. coli* type III asparaginase (PDB entry 3C17) T179A mutant cleavage site. T179* indicates a threonine modeled by us at this position. The distance from the Gly178 carbonyl carbon atom to the T179* hydroxyl group is 3.2 Å. (d) Overlay of the active site of hASNase3 uncleaved protomers from the substrate-free (green) and ASP-bound (magenta) structures. Residues N-terminal to Val169 adopt a slightly different conformation, showing the intrinsic flexibility of this region. (e) The hASNase3 fully cleaved protomer (tan) and uncleaved protomer from the partially cleaved (magenta) ASP-bound structures are superimposed. The double-headed arrow indicates the Gly9 flip upon cleavage.

that a conformational change is needed prior to this first step of the cleavage reaction. To gain insight into what this conformational change may be, we analyzed the structures of other asparaginases determined in the uncleaved state. In the case of the glycosylasparaginase from *Flavobacterium meningosepticum*, this required the use of the W11F mutant.³² In that structure, the distance between the threonine at the scissile

position (Thr152) and the carbon atom of the carbonyl group of the preceding residue is only 3.1 Å (Figure 6b; PDB entry 9GAF). Likewise, in the case of the *E. coli* type III asparaginase, obtaining the structure of the uncleaved state required the mutation of the critical threonine (Thr179) that was replaced with alanine.³¹ In that structure (Figure 6c; PDB entry 3c17), after first modeling a threonine side chain in place of the alanine (colored red in Figure 6c), we measured an analogous distance of 3.2 Å. The central difference between our uncleaved hASNase3 conformation, where the critical distance is too large (Figure 6a), and that in the uncleaved *F. meningosepticum* and *E. coli* structures, where that distance is more appropriate for a direct attack by the threonine hydroxyl group on the preceding residue's carbonyl group (Figure 6b,c), is the conformation of the peptide bond that precedes the threonine. Therefore, we suggest that for hASNase3 cleavage to occur, a conformational change in Gly167 is required, such that the distance between the carbonyl group and the Thr168 hydroxyl is shortened. This would necessitate flexibility in this part of the enzyme. Indeed, the conformation of this section differs in the two structures of the uncleaved protomers (Figure 6d), implying an intrinsic flexibility of the region that would allow for the required conformational change.

One of the few structural consequences of hASNase3 cleavage, from a single polypeptide to the α - and β -chains, is the flip in the conformation of Gly9, a residue in the spatial proximity of the cleavage site (double-headed arrow in Figure 6e). The conformation adopted by Gly9 in the postcleavage state would be incompatible with the conformation of Gly167 in the precleavage state (Figure 6e). In fact, the flip-in Gly9 conformation may act to promote the change in conformation of Gly167 to one that brings its carbonyl group closer to Thr168 and, in so doing, promotes the cleavage reaction. In conclusion, our structures suggest that the inherent flexibility of the cleavage region is required for the buildup of a cleavage-competent hASNase3 conformation.

Rationalizing the Substrate Specificity of hASNase3.

Enzymes such as human ASNase3 and AGA, in addition to being able to hydrolyze the free amino acid ASN, show hydrolytic activity with ASN derivatives. For example, hAGA's main function is to hydrolyze ASN-linked oligosaccharides in the lysosome, and hence its designation as aspartylglucosaminidase. In contrast, hASNase3 does not hydrolyze ASN-linked sugars but is able to hydrolyze isoaspartyl linkages.⁶ The shape of the active site cavities would dictate this difference in substrate specificity, prompting us to analyze the geometries of the active site entrance regions.

Common to both enzymes is the orientation of the minimal substrate, the amino acid ASN: the amino acid binds with its α -amino and carboxyl groups oriented toward the center of the protein, and with the side chain pointing out (Figure 7a–d). Divergence occurs with respect to the space possible for derivatives to extend from the ASN side chain. In the case of hASNase3, any molecule connected to the ASN side chain would most likely take one path (dotted black line in Figure 7b), whereas in hAGA, it would take an alternate path (dotted white line in Figure 7d). These paths are mutually exclusive because structural elements in one occupy the path most likely to be taken by the ASN derivative in the other. More specifically, residues present only in true asparaginases (such as *E. coli* type III asparaginase and hASNase3), and missing from aspartylglucosaminidases (such as hAGA), block the path that would be required for the sugar derivative (Figures S3 and S5

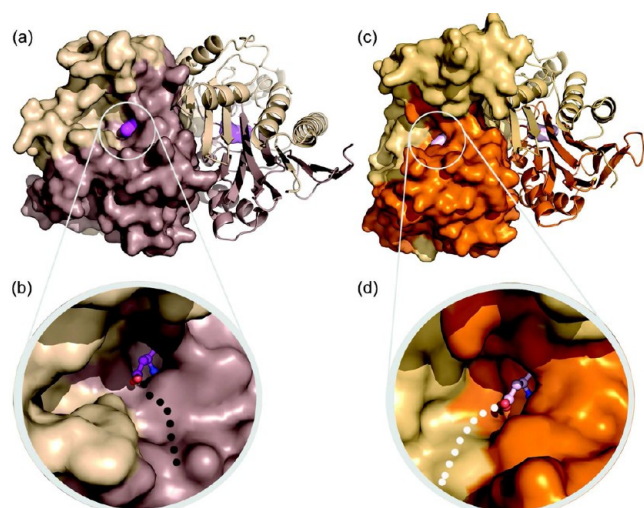


Figure 7. hASNase3 substrate specificity. The different substrate-binding cavities between hASNase3 and hAGA rationalize their distinctive substrate specificities for ASN derivatives. (a) The dimeric hASNase3 fully cleaved ASP complex is represented as a surface for protA and ribbon diagram for protB, colored in light and dark shades corresponding to the α - and β -chains, respectively. ASP is colored magenta. (b) Close-up of the hASNase3 active site entrance. ASP is represented in ball-and-stick mode, and the black dotted line indicates the space available for the ASN derivative moiety, such as a sugar or an aspartyl group. (c) Dimeric hAGA ASP complex (PDB entry 1APZ), represented as in panel a using light and dark orange shades for the α - and β -chains, respectively. ASP is colored pink. (d) Close-up of the hAGA active site entrance. ASP is represented in ball-and-stick mode, and the white dotted line indicates the space available for the ASN derivative moiety, such as a sugar or an aspartyl group. Note the difference in positioning of the cavity, and its larger size in hAGA.

of the Supporting Information). For example, hASNase3 differs from hAGA by having a long linker between β -strand A and α -helix 1 (for secondary structure labeling, see Figure 1b). Modeling of such a long linker (extra 16 residues) in hAGA demonstrates that this linker would block the space most likely to be required by the sugar moiety of an ASN sugar derivative (Figure S5 of the Supporting Information). This analysis illuminates the structural reasons behind the different substrate specificities of human ASNase3 and AGA.

CONCLUSIONS

Here, we present the crystal structures of amino acid-free and ASP-complexed human asparaginase 3, in both the uncleaved (inactive) and cleaved (active) states. The ASP complex structures, in addition to supplying a detailed view of the interactions between the enzyme and the product of the reaction, ASP, suggest that in the cleaved state, a direct interaction between the Thr168 amino and hydroxyl groups takes place. It is this interaction that would activate the Thr168 hydroxyl group for attack on the side chain of the substrate ASN. The slow intrinsic autocleavage rate of hASNase3 allowed us to observe the uncleaved state without resorting to cleavage-inactivating mutations. The structures also suggest a role for the conserved N-terminal segment (His8–Gly9) in promoting the cleavage-competent conformation, a feature not noted previously for other members of this enzyme family. Any modifications to hASNase3 done for the purpose of lowering its ASN K_m value, to allow it to act as a replacement for bacterial asparaginases in blood cancer therapy, would need to take these

aspects into consideration, to still permit the essential intramolecular cleavage reaction.

ASSOCIATED CONTENT

Supporting Information

Overlay of the cleaved and uncleaved hASNase3 with a close-up of the active site (Figure S1), overlay of the cleaved and uncleaved hASNase3 with a close-up of the His8–Gly10 loop that changes conformation (Figure S2), sequence alignment of type III asparaginases (Figure S3), comparison of hASNase3 to the *E. coli* and hAGA enzymes (Figure S4), and surface representation of hAGA with the hASNase3 strand A–helix 1 overlaid demonstrating the structural reasons for the different substrate specificity (Figure S5). This material is available free of charge via the Internet at <http://pubs.acs.org>.

AUTHOR INFORMATION

Corresponding Author

*E-mail: lavie@uic.edu. Telephone: (312) 355-5029. Fax: (312) 355-4535.

Funding

This work was supported by National Institutes of Health Grant R21 CA155424 and the Max Planck Society.

Notes

The authors declare no competing financial interest.

ACKNOWLEDGMENTS

We thank the University of Illinois at Chicago's Research Resources Center and in particular Bernard Santarsiero for assistance with the in-house X-ray equipment. We also thank the three anonymous reviewers for their constructive comments.

ABBREVIATIONS

hASNase3, hASRGL1; Ntn, N-terminal nucleophile; hAGA, human aspartylglucosaminidase; rmsd, root-mean-square deviation.

REFERENCES

- (1) Sugimoto, H., Odani, S., and Yamashita, S. (1998) Cloning and expression of cDNA encoding rat liver 60-kDa lysophospholipase containing an asparaginase-like region and ankyrin repeat. *J. Biol. Chem.* 273, 12536–12542.
- (2) Menniti, M., Iuliano, R., Foller, M., Sopjani, M., Alesutan, I., Mariggio, S., Nofziger, C., Perri, A. M., Amato, R., Blazer-Yost, B., Corda, D., Lang, F., and Perrotti, N. (2010) 60 kDa lysophospholipase, a new Sgk1 molecular partner involved in the regulation of ENaC. *Cell. Physiol. Biochem.* 26, 587–596.
- (3) Mononen, I., Fisher, K. J., Kaartinen, V., and Aronson, N. N., Jr. (1993) Aspartylglycosaminuria: Protein chemistry and molecular biology of the most common lysosomal storage disorder of glycoprotein degradation. *FASEB J.* 7, 1247–1256.
- (4) Bush, L. A., Herr, J. C., Wolkowicz, M., Sherman, N. E., Shore, A., and Flickinger, C. J. (2002) A novel asparaginase-like protein is a sperm autoantigen in rats. *Mol. Reprod. Dev.* 62, 233–247.
- (5) Evtimova, V., Zeillinger, R., Kaul, S., and Weidle, U. H. (2004) Identification of CRASH, a gene deregulated in gynecological tumors. *Int. J. Oncol.* 24, 33–41.
- (6) Cantor, J. R., Stone, E. M., Chantarnupong, L., and Georgiou, G. (2009) The human asparaginase-like protein 1 hASRGL1 is an Ntn hydrolase with β -aspartyl peptidase activity. *Biochemistry* 48, 11026–11031.

- (7) Aswad, D. W., Paranandi, M. V., and Schurter, B. T. (2000) Isoaspartate in peptides and proteins: Formation, significance, and analysis. *J. Pharm. Biomed. Anal.* 21, 1129–1136.
- (8) Brannigan, J. A., Dodson, G., Duggleby, H. J., Moody, P. C., Smith, J. L., Tomchick, D. R., and Murzin, A. G. (1995) A protein catalytic framework with an N-terminal nucleophile is capable of self-activation. *Nature* 378, 416–419.
- (9) Galperin, M. Y., and Koonin, E. V. (2012) Divergence and convergence in enzyme evolution. *J. Biol. Chem.* 287, 21–28.
- (10) Borek, D., and Jaskolski, M. (2000) Crystallization and preliminary crystallographic studies of a new L-asparaginase encoded by the *Escherichia coli* genome. *Acta Crystallogr. D* 56, 1505–1507.
- (11) Verma, N., Kumar, K., Kaur, G., and Anand, S. (2007) L-Asparaginase: A promising chemotherapeutic agent. *Crit. Rev. Biotechnol.* 27, 45–62.
- (12) Swain, A. L., Jaskolski, M., Housset, D., Rao, J. K., and Wlodawer, A. (1993) Crystal structure of *Escherichia coli* L-asparaginase, an enzyme used in cancer therapy. *Proc. Natl. Acad. Sci. U.S.A.* 90, 1474–1478.
- (13) Michalska, K., and Jaskolski, M. (2006) Structural aspects of L-asparaginases, their friends and relations. *Acta Biochim. Pol.* 53, 627–640.
- (14) Appel, I. M., Kazemier, K. M., Boos, J., Lanvers, C., Huijman, J., Veerman, A. J., van Wering, E., den Boer, M. L., and Pieters, R. (2008) Pharmacokinetic, pharmacodynamic and intracellular effects of PEG-asparaginase in newly diagnosed childhood acute lymphoblastic leukemia: Results from a single agent window study. *Leukemia* 22, 1665–1679.
- (15) Avramis, V. I., and Tiwari, P. N. (2006) Asparaginase (native ASNase or pegylated ASNase) in the treatment of acute lymphoblastic leukemia. *Int. J. Nanomed.* 1, 241–254.
- (16) Ellem, K. A., Fabrizio, A. M., and Jackson, L. (1970) The dependence of DNA and RNA synthesis on protein synthesis in asparaginase-treated lymphoma cells. *Cancer Res.* 30, 515–527.
- (17) Gong, S. S., and Basilico, C. (1990) A mammalian temperature-sensitive mutation affecting G1 progression results from a single amino acid substitution in asparagine synthetase. *Nucleic Acids Res.* 18, 3509–3513.
- (18) Ueno, T., Ohtawa, K., Mitsui, K., Kadera, Y., Hiroto, M., Matsushima, A., Inada, Y., and Nishimura, H. (1997) Cell cycle arrest and apoptosis of leukemia cells induced by L-asparaginase. *Leukemia* 11, 1858–1861.
- (19) Armstrong, J. K., Hempel, G., Koling, S., Chan, L. S., Fisher, T., Meiselman, H. J., and Garratty, G. (2007) Antibody against poly(ethylene glycol) adversely affects PEG-asparaginase therapy in acute lymphoblastic leukemia patients. *Cancer* 110, 103–111.
- (20) Kabsch, W. (1993) Automatic processing of rotation diffraction data from crystals of initially unknown symmetry and cell constants. *J. Appl. Crystallogr.* 24, 795–800.
- (21) Vagin, A., and Teplyakov, A. (1997) MOLREP: An automated program for molecular replacement. *J. Appl. Crystallogr.* 30, 1022–1025.
- (22) Murshudov, G. N., Vagin, A. A., and Dodson, E. J. (1997) Refinement of macromolecular structures by the maximum-likelihood method. *Acta Crystallogr. D* 53, 240–255.
- (23) Krissinel, E., and Henrick, K. (2007) Inference of macromolecular assemblies from crystalline state. *J. Mol. Biol.* 372, 774–797.
- (24) Xuan, J., Tarentino, A. L., Grimwood, B. G., Plummer, T. H., Jr., Cui, T., Guan, C., and Van Roey, P. (1998) Crystal structure of glycosylasparaginase from *Flavobacterium meningosepticum*. *Protein Sci.* 7, 774–781.
- (25) Michalska, K., Bujacz, G., and Jaskolski, M. (2006) Crystal structure of plant asparaginase. *J. Mol. Biol.* 360, 105–116.
- (26) Wang, Y., and Guo, H. C. (2010) Crystallographic snapshot of glycosylasparaginase precursor poised for autoprocessing. *J. Mol. Biol.* 403, 120–130.
- (27) Oinonen, C., Tikkanen, R., Rouvinen, J., and Peltonen, L. (1995) Three-dimensional structure of human lysosomal aspartylglucosaminidase. *Nat. Struct. Biol.* 2, 1102–1108.
- (28) Tikkanen, R., Riikonen, A., Oinonen, C., Rouvinen, R., and Peltonen, L. (1996) Functional analyses of active site residues of human lysosomal aspartylglucosaminidase: Implications for catalytic mechanism and autocatalytic activation. *EMBO J.* 15, 2954–2960.
- (29) Guo, H. C., Xu, Q., Buckley, D., and Guan, C. (1998) Crystal structures of *Flavobacterium* glycosylasparaginase. An N-terminal nucleophile hydrolase activated by intramolecular proteolysis. *J. Biol. Chem.* 273, 20205–20212.
- (30) Prahl, A., Pazgier, M., Hejazi, M., Lockau, W., and Lubkowski, J. (2004) Structure of the isoaspartyl peptidase with L-asparaginase activity from *Escherichia coli*. *Acta Crystallogr. D* 60, 1173–1176.
- (31) Michalska, K., Hernandez-Santoyo, A., and Jaskolski, M. (2008) The mechanism of autocatalytic activation of plant-type L-asparaginases. *J. Biol. Chem.* 283, 13388–13397.
- (32) Xu, Q., Buckley, D., Guan, C., and Guo, H. C. (1999) Structural insights into the mechanism of intramolecular proteolysis. *Cell* 98, 651–661.